Electronic Supplementary Information

Crosstalk Free Graphene-Liquid Elastomer Based Printed Sensor for Unobtrusive Respiratory Monitoring

Simran Sharma,[a] Ankur Thapa[a], Sumit Singh,[b] Titash Mondal[a*]

[a] *Rubber Technology Centre, Indian Institute of Technology Kharagpur, Kharagpur, India-721302*

[b] *Anton Paar India Pvt. Ltd., Gurgaon, India-122016*

Corresponding Author: titash@rtc.iitkgp.ac.in

(a)

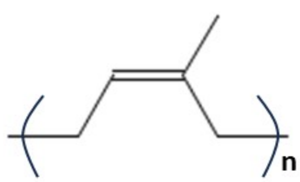

(b)

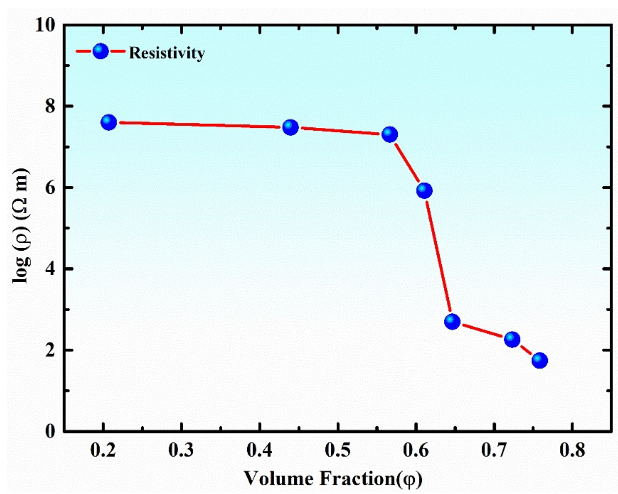

Fig. S1: (a) polyisoprene unit **(b)** Electrical resistivity plot for different composition against the filler volume fraction

Table S1: Conductivity and standard deviation for different volume fraction samples

Volume Fraction	Log (σ)	Std Deviation (3 samples)
0.21	-7.60206	0.147
0.44	-7.47712	0.125
0.56	-7.30103	0.167
0.61	-5.91908	0.165
0.67	-2.69897	0.100
0.72	-2.26007	0.115

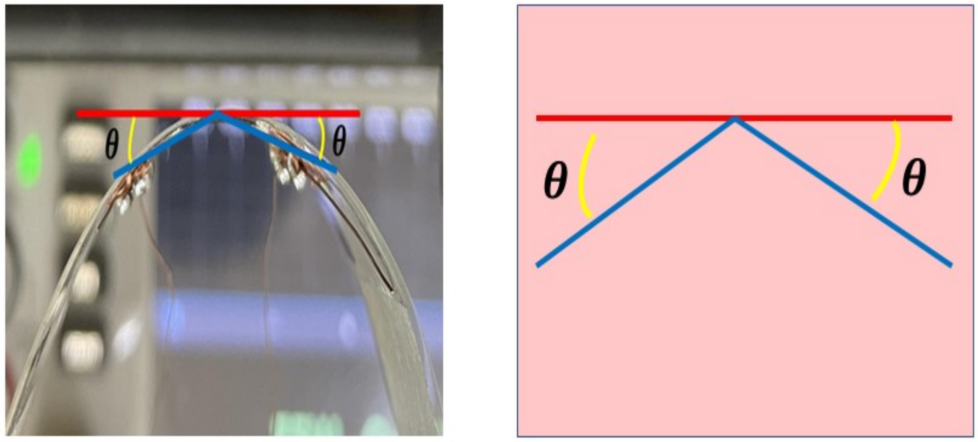

Fig. S2: Bending of the samples at different angles using the in house fabricated device.

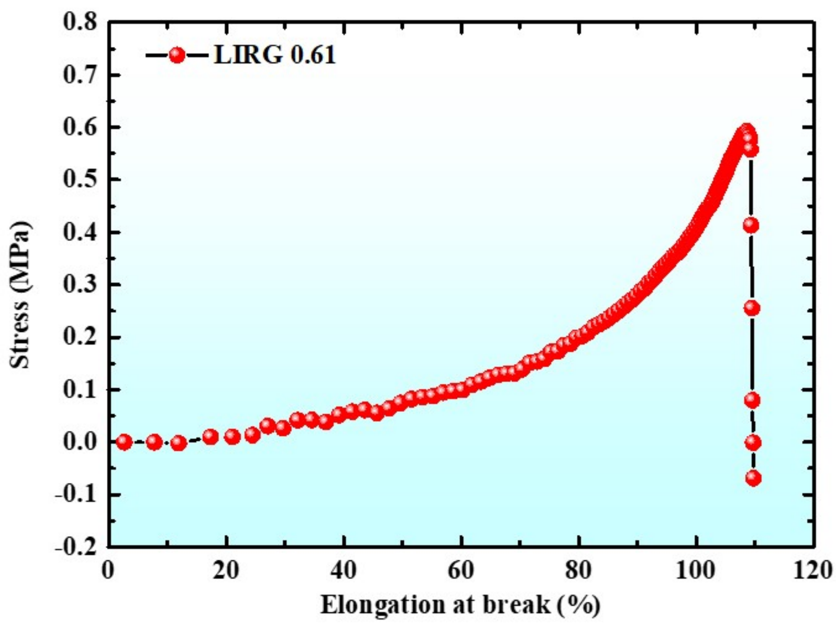

Fig. S3: Tensile strength and Elongation at Break for LIRG 0.61 sensor

Fig. S4: N 95 mask attached with the LIRG 0.61 sample.

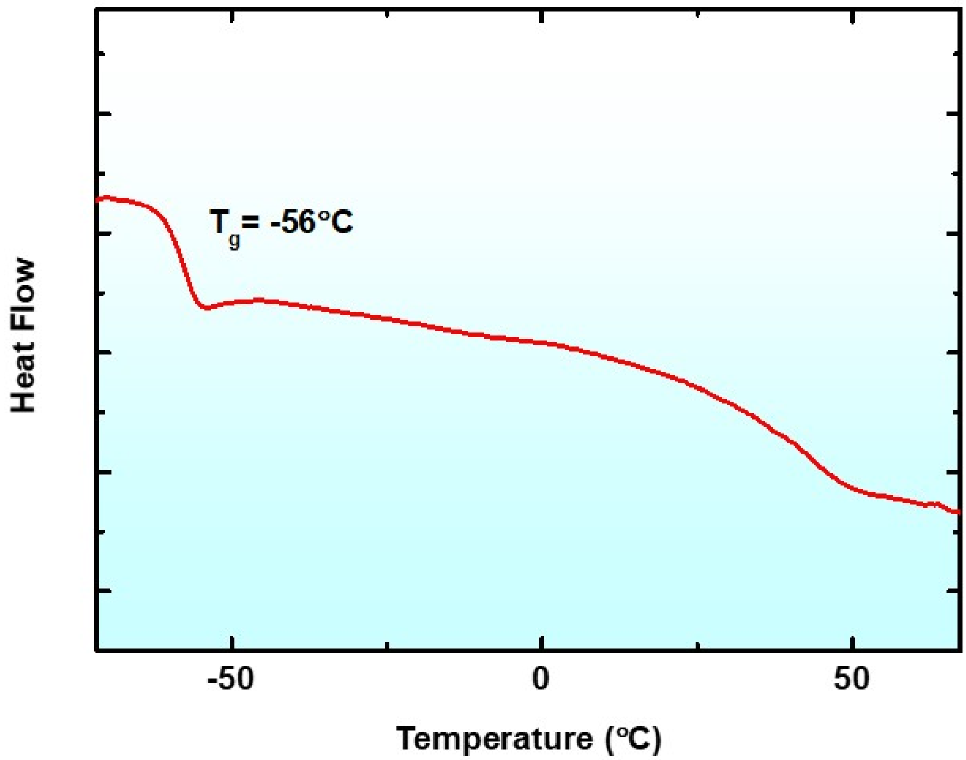

Fig. S5: DSC trace of the LIRG 0.61 sample.

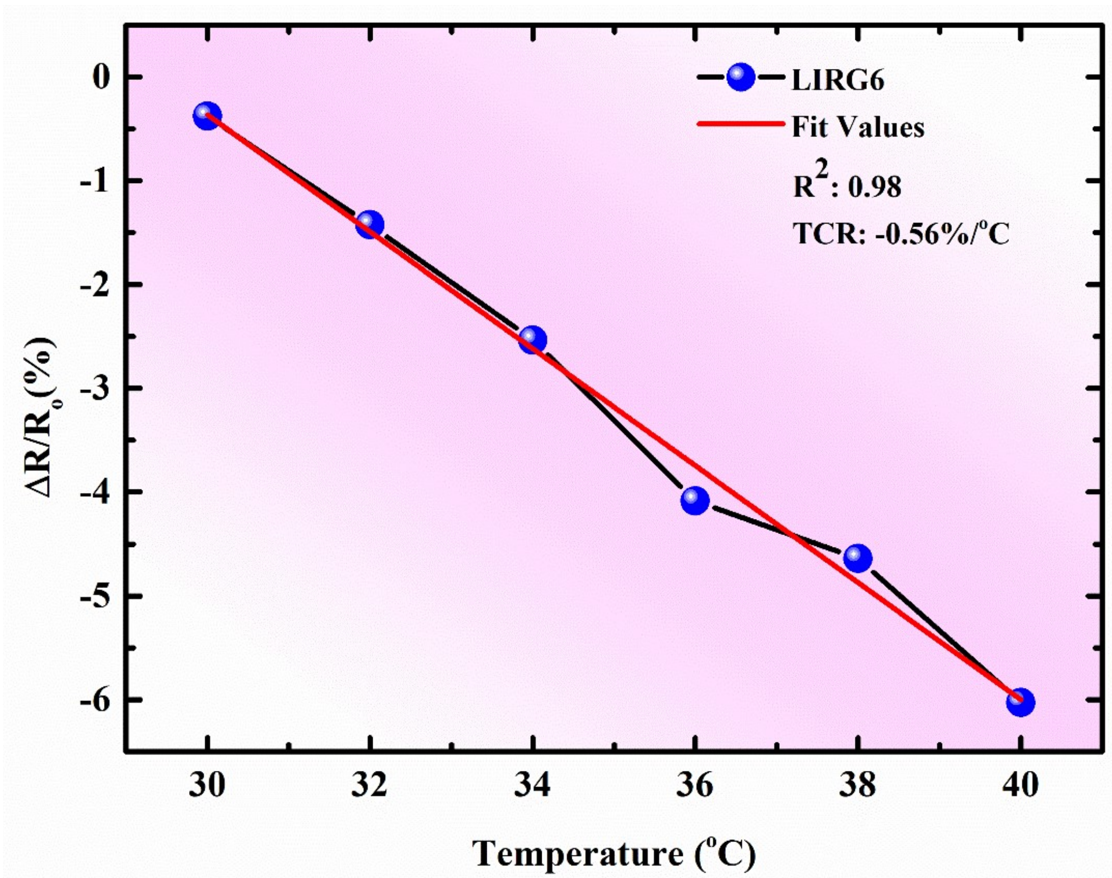

Fig. S6: Thermal sensitivity of LIRG 0.61 sensor.

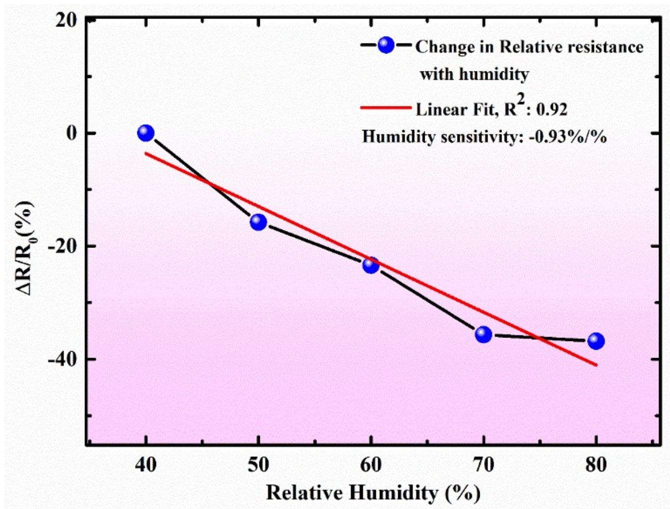

Fig. S7: Impact of Humidity on the LIRG 0.61 sample

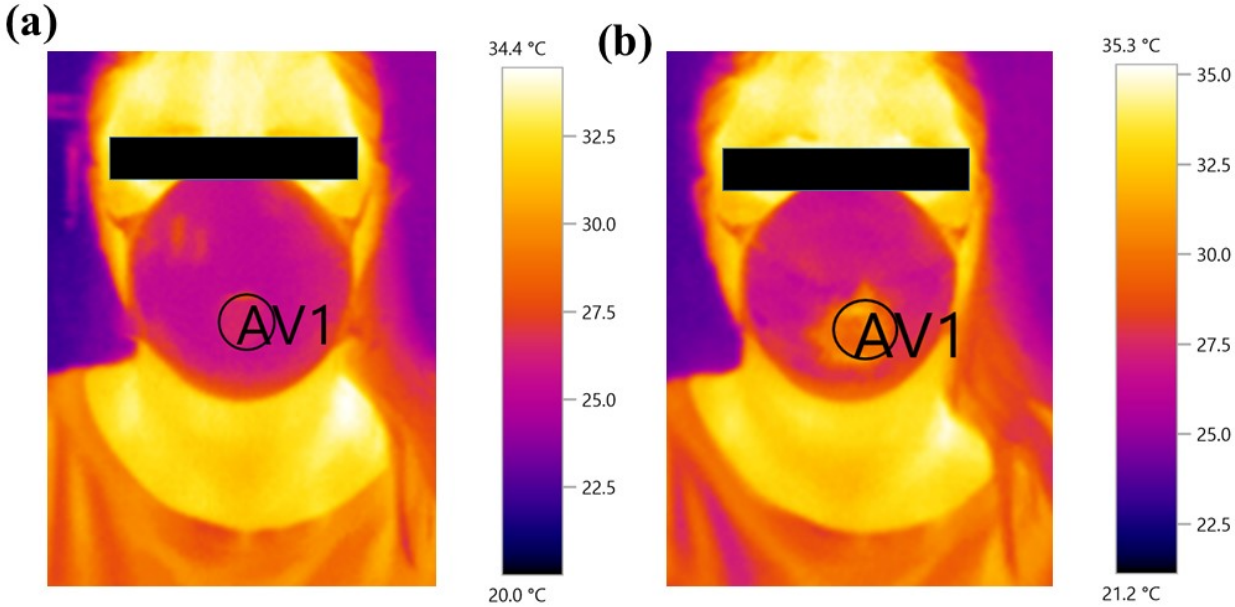

Fig. S8: Infra-red image of the mask during **(a)** inhalation, and **(b)** exhalation demonstrating the increase in temperature during the breathing.

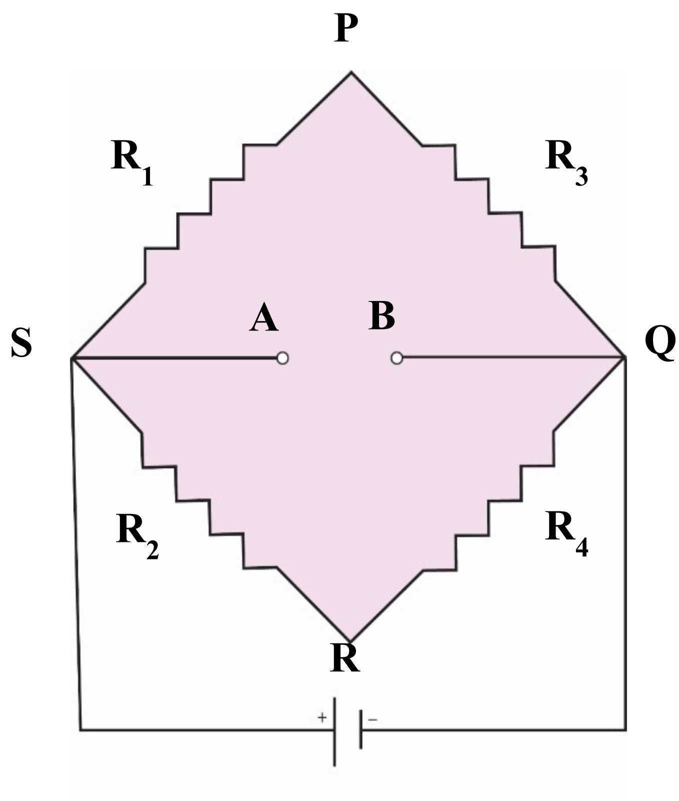

Fig. S9: Wheatstone bridge arrangement for the sensors

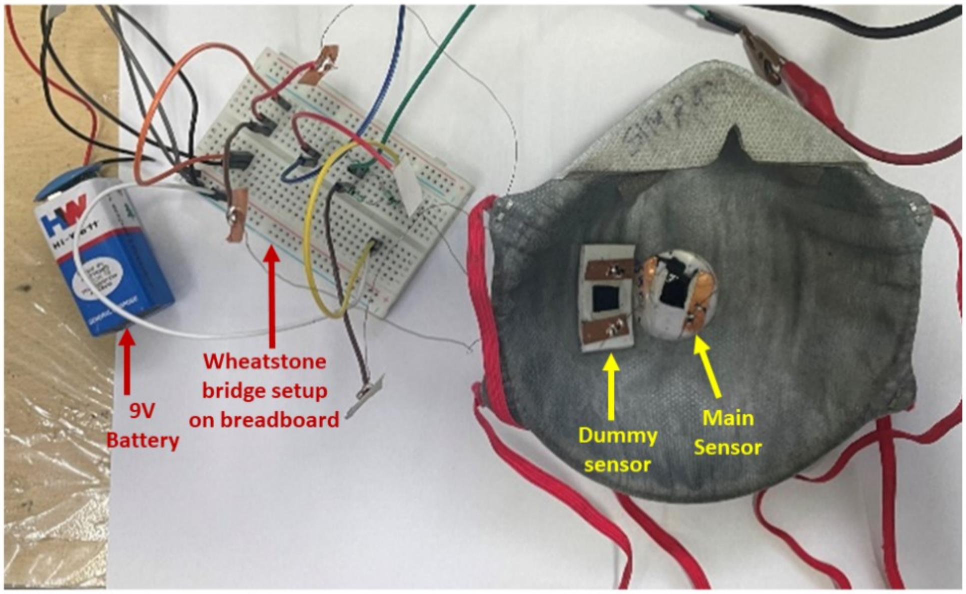

Fig. S10: Wheatstone bridge arrangement for the sensors over the mask

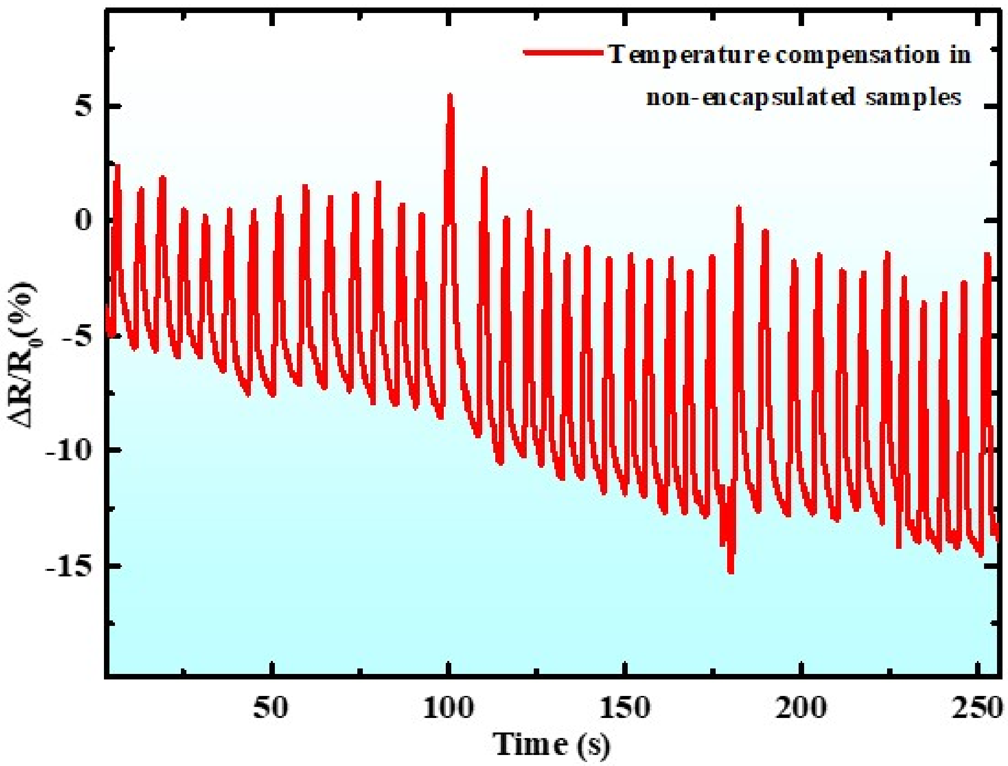

Fig. S11: Temperature-compensated signal output for non-encapsulated samples

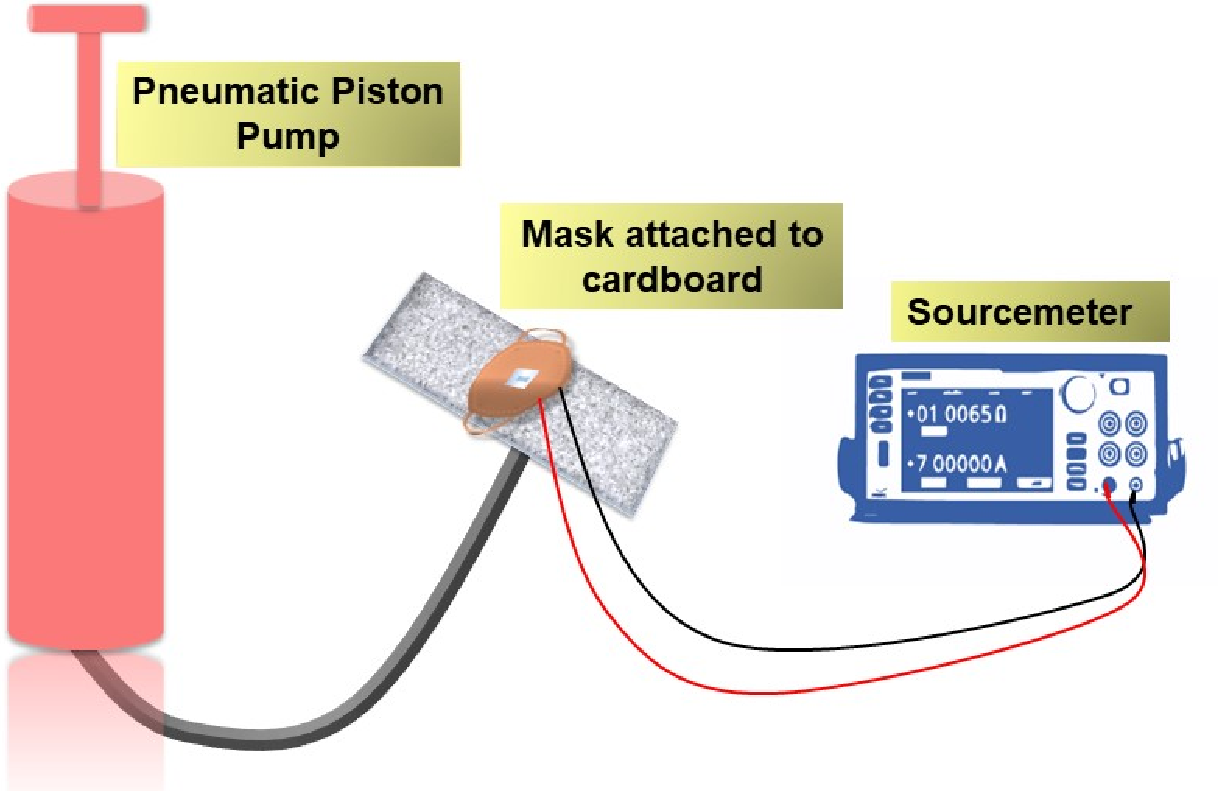

Fig. S12: Simulated breathing on mask set-up with the aid of air pump

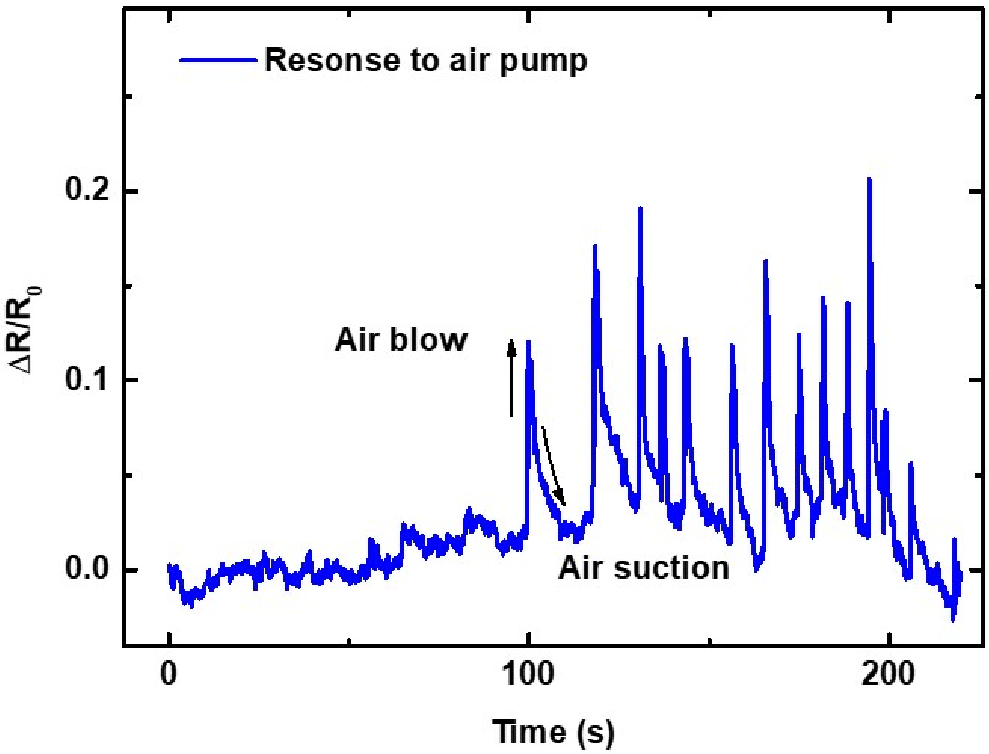

Fig. S13: Relative resistance change with simulated breathing experiment

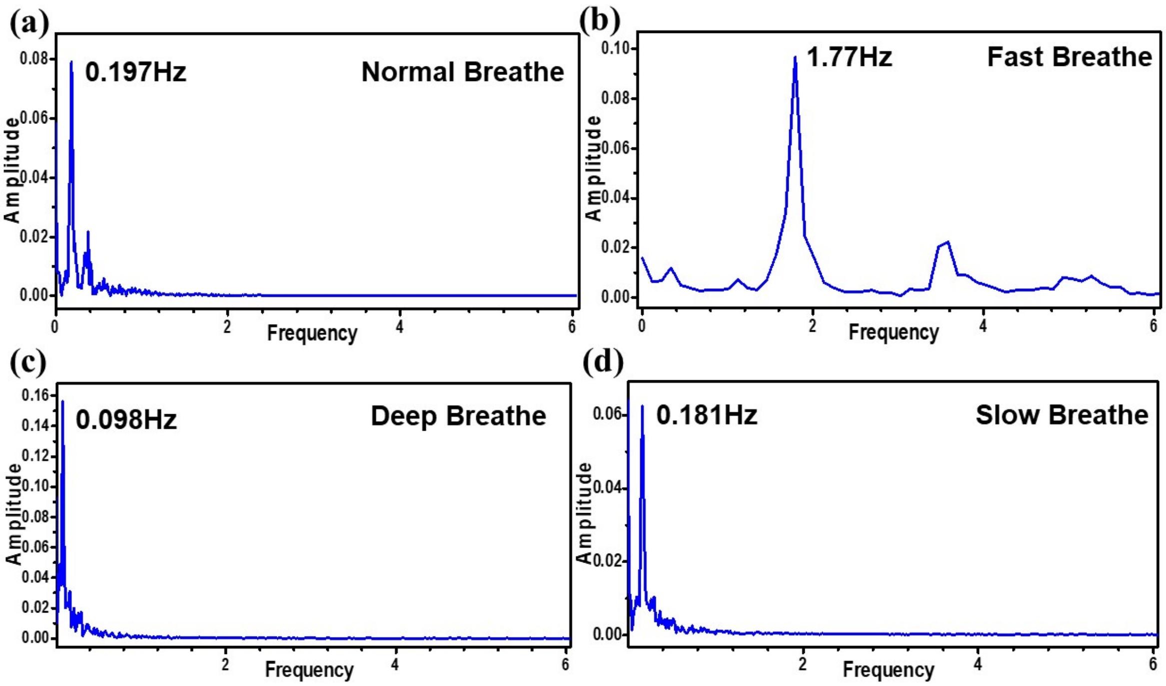

Fig. S14. Fast Fourier Transform (FFT) of the transformed signals respectively for (a) Normal, (b) fast, (c) deep and (d) fast breathing.

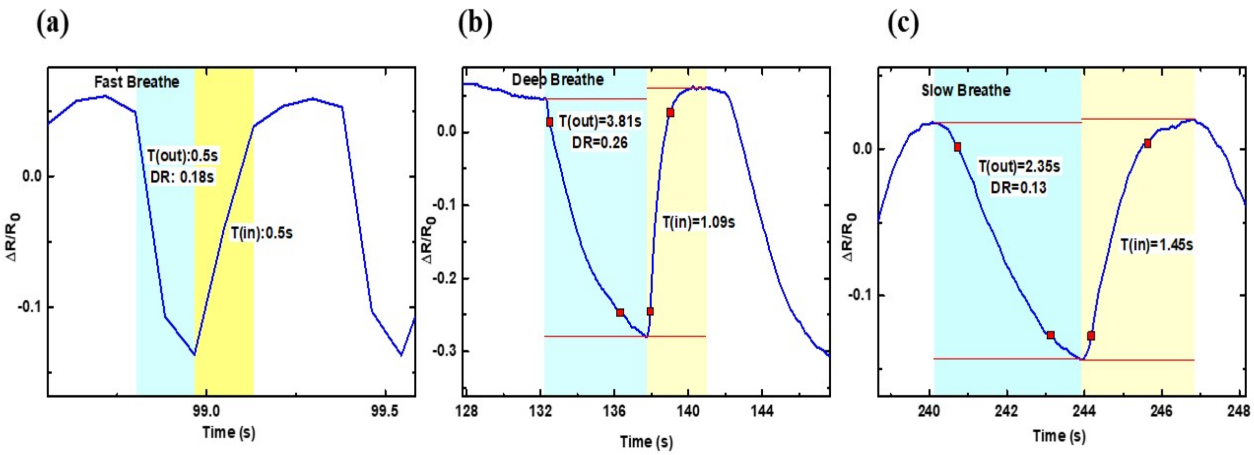

Fig. S15: Expanded breathing signal obtained after the application of encapsulant and wheatstone bridge for fast, deep and slow breathing.

Table S2: Quantitative analysis of breathing parameters before and after the removal of cross-talk

Breathing Type	RR	Average DR	T_{in}	T_{out}	Total Breath Time	(I:E)= T_{in}:T_{out}	SNR
Normal (After Encapsulation & Wheatsone bridge application)	12	0.18	0.72	2.48	3.2	1:3.4	-12.85
Normal (Before Encapsulation & Wheatstone bridge application)	13	0.059	0.65	0.44	1.09	1.5:1	-21.48

Table S3: Comparative analysis of I:E from the literature

Breathing Type	T_{in}	T_{out}	(I:E)= T_{in}/T_{out}
Reference [1]	630ms	730ms	0.86
Reference [2]	-	-	0.8
Reference [3]	0.88	1.178	0.74
This work (before cross-talk removal)	0.65	0.44	1.47
This work (After cross-talk removal)	0.72s	2.4s	0.29

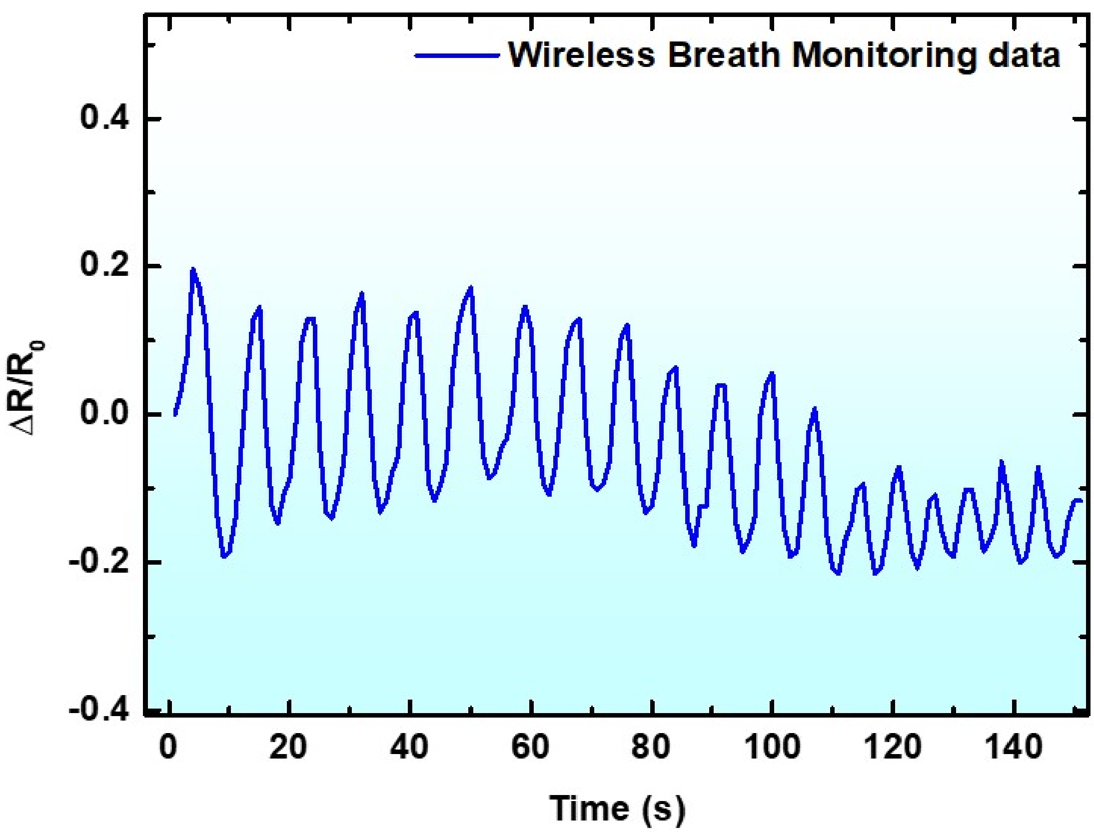

Fig. S16: Plot of wireless monitoring signal data received via. Bluetooth module onto the smartphone.

Table S4: Comparative analysis of mask-based respiratory sensors

S.No.	Mask-based Sensing Mechanism	Sensing Material	Fabrication Route	Sub-ambient Respiration monitoring	Sensitivity	Solvent Used	Reference
1	Humidity	$CsPbBr_3$	Spin-coating	No	1.5565%/RH%	Yes	[4]
2	Triboelectric	Acrylonitrile butadiene styrene	3D printing	No	Upto 6.614 nA/KPa	No	[5]
3	Humidity	Graphdiyne	Spray Printing	No	140% ($\Delta I/I_0$)	Yes	[1]
4	Humidity	Carbon nanotubes	Ultrasonication assisted anchoring	No	$<\Delta R/R_0\%=30$ at 95% RH	Yes	[6]
5	Humidity	Copper wire/Coolmax yarn/ PENTAS yarn/ Cleancool yarn/ polyimide yarn	Yarn ply	No	Upto 82.40 pF/ % RH	No	[7]
6	Humidity	Mxene/MWCNT	Drop coating	No	<Response %=250% at 90%RH	Yes	[2]
7	Temperature	Cr/Au/PDMS	Photolithography/Spin casting	No	Thermal index= 3786K	Yes	[8]
8	Pressure	Graphene	Solution casting	No	Upto 17.2 kPa^{-1} in range 0-20 kPa	Yes	[9]
9	Pressure	MXene	Screen printing	No	509.5 or 344.0 kPa^{-1}, a low limit (~1 Pa) & (100 kPa)	Yes	[10]
10	Strain	Graphene/carbon black/SWCNT	Dip Coating	No	Guage factor= 2.14 in range 0-100% strain	Yes	[11]
11	Strain	Graphene	Stencil Printing	Yes	Guage factor= -196.56 (0-0.17 %) strain and 117.49 in (0.17-0.34 %) strain region	No	This work

References

(1) Li, Y.; Zhang, M.; Hu, X.; Yu, L.; Fan, X.; Huang, C.; Li, Y. Graphdiyne-Based Flexible Respiration Sensors for Monitoring Human Health. *Nano Today* **2021**, *39*. https://doi.org/10.1016/j.nantod.2021.101214

(2) Xing, H.; Li, X.; Lu, Y.; Wu, Y.; He, Y.; Chen, Q.; Liu, Q.; Han, R. P. S. MXene/MWCNT Electronic Fabric with Enhanced Mechanical Robustness on Humidity Sensing for Real-Time Respiration Monitoring. *Sens Actuators B Chem* **2022**, *361*. https://doi.org/10.1016/j.snb.2022.131704.

(3) Thiyagarajan, K.; Rajini, R. K.; Maji, D.; Flexible, highly sensitive Paper-based Screen Printed MWCNT/PDMS Composite Breath Sensor for Human Respiratory Monitoring **2021**. IEEE Sensors J. 21(13), 13985 – 13995. https://doi.org/ 10.1109/JSEN.2020.3040995

(4) Wu, Z.; Yang, J.; Sun, X.; Wu, Y.; Wang, L.; Meng, G.; Kuang, D.; Guo, X. Z.; Qu, W.; Du, B.; Liang, C.; Fang, X.; Tang, X.; He, Y. An Excellent Impedance-Type Humidity Sensor Based on Halide Perovskite CsPbBr3 Nanoparticles for Human Respiration Monitoring. *Sens Actuators B Chem* **2021**, *337*. https://doi.org/10.1016/j.snb.2021.129772.

(5) Yun, J.; Park, J.; Jeong, S.; Hong, D.; Kim, D. A Mask-Shaped Respiration Sensor Using Triboelectricity and a Machine Learning Approach toward Smart Sleep Monitoring Systems. *Polymers (Basel)* **2022**, *14* (17). https://doi.org/10.3390/polym14173549.

(6) Huang, X.; Li, B.; Wang, L.; Lai, X.; Xue, H.; Gao, J. Superhydrophilic, Underwater Superoleophobic, and Highly Stretchable Humidity and Chemical Vapor Sensors for Human Breath Detection. *ACS Appl Mater Interfaces* **2019**, *11* (27), 24533–24543. https://doi.org/10.1021/acsami.9b04304.

(7) Ma, L.; Wu, R.; Patil, A.; Zhu, S.; Meng, Z.; Meng, H.; Hou, C.; Zhang, Y.; Liu, Q.; Yu, R.; Wang, J.; Lin, N.; Liu, X. Y. Full-Textile Wireless Flexible Humidity Sensor for Human Physiological Monitoring. *Adv Funct Mater* **2019**, *29* (43). https://doi.org/10.1002/adfm.201904549.

(8) Liu, Y.; Zhao, L.; Avila, R.; Yiu, C.; Wong, T.; Chan, Y.; Yao, K.; Li, D.; Zhang, Y.; Li, W.; Xie, Z.; Yu, X. Epidermal Electronics for Respiration Monitoring via Thermo-Sensitive Measuring. *Materials Today Physics* **2020**, *13*. https://doi.org/10.1016/j.mtphys.2020.100199.

(9) Tao, L. Q.; Zhang, K. N.; Tian, H.; Liu, Y.; Wang, D. Y.; Chen, Y. Q.; Yang, Y.; Ren, T. L. Graphene-Paper Pressure Sensor for Detecting Human Motions. *ACS Nano* **2017**, *11* (9), 8790–8795. https://doi.org/10.1021/acsnano.7b02826.

(10) Yang, L.; Wang, H.; Yuan, W.; Li, Y.; Gao, P.; Tiwari, N.; Chen, X.; Wang, Z.; Niu, G.; Cheng, H. Wearable Pressure Sensors Based on MXene/Tissue Papers for Wireless Human Health Monitoring. *ACS Appl Mater Interfaces* **2021**, *13* (50), 60531–60543. https://doi.org/10.1021/acsami.1c22001.

(11) Huang, Y.; Zhao, Y.; Wang, Y.; Guo, X.; Zhang, Y.; Liu, P.; Liu, C.; Zhang, Y. Highly Stretchable Strain Sensor Based on Polyurethane Substrate Using Hydrogen Bond-Assisted Laminated Structure for Monitoring of Tiny Human Motions. *Smart Mater Struct* **2018**, *27* (3). https://doi.org/10.1088/1361-665X/aaaba0.